SCIENTIFIC REPORTS

OPEN

SUBJECT AREAS:
MOLECULAR ECOLOGY
ECOLOGICAL GENETICS

Received
15 August 2014

Accepted
30 December 2014

Published
27 January 2015

Correspondence and requests for materials should be addressed to X.-Y.H. (xyhong@njau.edu.cn)

Evidence for high dispersal ability and mito-nuclear discordance in the small brown planthopper, *Laodelphax striatellus*

Jing-Tao Sun[1], Man-Man Wang[1], Yan-Kai Zhang[1], Marie-Pierre Chapuis[2], Xin-Yu Jiang[1], Gao Hu[1], Xian-Ming Yang[1], Cheng Ge[1], Xiao-Feng Xue[1] & Xiao-Yue Hong[1]

[1]Department of Entomology, Nanjing Agricultural University, Nanjing, Jiangsu 210095, China, [2]CIRAD, UMR CBGP, F-34398 Montpellier, France.

Understanding dispersal ability in pest species is critical for both theoretical aspects of evolutionary and population biology and from a practical standpoint, such as implementing effective forecasting systems. The small brown planthopper (SBPH), *Laodelphax striatellus* (Fallén), is an economically important pest, but few data exist on its dispersal ability. Here, we used mitochondrial and nuclear markers to elucidate the population genetic structure of SBPH and of the parasitic bacterium *Wolbachia* throughout temperate and subtropical China. Our results showed that the SBPH populations in China lack significant differences in genetic structure, suggesting extensive gene flow. Multilocus sequence typing revealed that *Wolbachia* infection was systematic and due to the same strain (*w*Stri) within and across populations. However, the mtDNA haplogroups had a nonrandom distribution across the sampling localities, which correlated to latitudinal and climatic gradients. We explain this mito-nuclear discordance as a result of historical population recolonization or mitochondria adaptation to climate.

Dispersal not only has important consequences for the spatial and temporal dynamics of populations, but also affects gene frequencies and the relative importance of a given species in the local community[1]. Dispersal also helps an organism to cope with environmental changes by allowing it to colonize more suitable habitats[2]. Besides its ecological importance, dispersal has effects on evolutionary processes. For example, speciation depends on a balance between local adaptation and dispersal[3]. Consequently, measuring dispersal is a focus of research in evolutionary biology, conservation biology and pest management.

For pest species, quantifying dispersal is not only key to resolving questions related to pests' behavioral traits, and physiological or genetic constraints, but also to developing a forecasting system for integrated pest management plans[4]. A case in hand is the small brown planthopper (SBPH), *Laodelphax striatellus* (Fallén), a notorious agricultural pest, which is widely distributed from the Philippines to Siberia and Europe, mainly in the temperate zone. SBPH not only causes sucking damage to crops but also spreads the damaging plant disease *Rice stripe virus* (RSV)[5]. The most recent outbreak of RSV in eastern China in 2000 caused significant losses[6]. RSV is strictly transmitted by SBPH in persistent propagative and transovarial manners[6]. Therefore, the dispersal ability of SBPH plays a critical role in shaping the population structure of RSV. Sometimes, it is unclear whether the outbreak of RSV was triggered by local strains or invasive strains associated with the dispersal of SBPH. Understanding the dispersal pattern of SBPH is therefore not only key to developing effective control strategies for this pest, but also has implications for the ecology and evolution of vector-borne RSV virus systems, as well as for RSV epidemiology and control.

Two alternative views exist on the importance of dispersal in SBPH population dynamics. The common view is that outbreaks are caused by local resident populations[7]. Unlike the other two rice planthoppers, brown planthoppers (*Nilaparvata lugens*) and white-backed planthoppers (*Sogatella furcifera*), SBPH is able to overwinter by diapausing as third- or fifth-instar nymphs in temperate climates[8], including all regions of China, and no seasonal migration is required between climatic areas of the species range[7]. Moreover, SBPH populations display geographic differences in the critical day length to induce larval diapause and in the diapause depth[9]. If genetically-induced, such life history variation among SBPH populations would suggest local adaptation to climate and

limited gene flow between populations. This is supported by a population genetic structure of SBPH in Japan based on three allozyme loci which reveal significant differentiation between populations[9].

An alternative view is that outbreaks are caused by long-distance migration events. Potential to migrate is indicated by catches of a considerable number of SBPH at high altitudes or over the sea with *N. lugens* and *S. furcifera*, two species which annually migrate to China from the Indochina Peninsula riding the air currents in the early spring[10,11]. Moreover, a comparison of insecticide susceptibility between Chinese and Japanese populations coupled with a backward trajectory analysis indicated that SBPH can fly from China to Japan[12]. Accordingly, extensive gene flow between populations was suggested by a phylogenetic analysis in China based on a fragment of the Cytochrome C Oxidase Subunit *II* (*COII*), which showed that identical or highly similar haplotypes were shared between different geographic populations[13]. These observations suggest that SBPH, like *N. lugens* and *S. furcifera*, is able to migrate long distances.

Conventional methods for studying the movement of insects include fluorescent marker dyes and radio-isotopes. However, these methods are difficult to apply to SBPH because of their small size, short lifespan, large population sizes, and rapid aerial population dilution[14]. An indirect approach is to use molecular markers that will give us access to genetic parameters partially linked to actual demographic parameters. Genetic structure inferred from molecular markers reflects the interaction of genetic drift, mutation, migration and selection, with influences from life history. For example, highly migratory species are usually expected to have low genetic differentiation and minimal population structure because of strong gene flow. In spite of the difficult challenge of linking genetics and demographic population parameters[15], population genetics have been successfully employed to elucidate the flight behavior or migratory ability of a range of insect species[16–18]. However, there is not yet any conclusive evidence for the population genetic structure of SBPH. The molecular markers (allozymes or *COII* gene), numbers of samples (9∼281) and sample types (laboratory reared populations or natural populations) used in previous studies have led to contradictory results and limited ability to reveal the reliable pattern of its population structure[9,13].

Furthermore, by its influence in shaping host population genetics, infection by the endosymbiotic bacterium *Wolbachia*, which is common in SBPH[9,19], may at least partially explain the contradictory results of previous studies. *Wolbachia* is a maternally inherited alpha-proteobacteria and induces cytoplasmic incompatibility (CI) in SBPH, a mechanism by which mating between uninfected females and infected males results in no offspring. However, the infected females can mate with both the infected and uninfected males, and produce offsprings successfully. The CI level of SBPH is quite high and even old males strongly cause CI[20]. Because of the reproductive advantage of *Wolbachia*-infected females, even a small number of *Wolbachia*-infected insects can lead to a rapid spread and fixation of the infection. In association with *Wolbachia* spread, a small number of mitochondrial haplotypes borne by infected individuals are also spread within populations, reducing the mitochondrial diversity of populations[21,22]. Moreover, CI can prevent gene flow from infected to uninfected populations, promoting genetic divergence[23], and has attracted attention as a possible mechanism for rapid speciation[23–25]. Thus, the high CI level in SBPH can bias measurements of diversity and structure estimated by mtDNA markers in its populations. However, if complemented with data from nuclear markers, the effect of CI on the population structure of its host can be assessed and controlled. Simultaneously, the *Wolbachia* infection status (infection frequencies and *Wolbachia* strains) of different SBPH geographic populations *per se* will provide information on the population structure and dispersal ability.

In this study, we set out to explore the following two questions: (1) Does SBPH show evidence of a high level of dispersal from population genetic data? If this is the case, we expect a low level of genetic differentiation between populations and no isolation-by-distance effect. (2) Does *Wolbachia* affect the mitochondrial DNA genetic diversity and structure of SBPH populations? If this is the case, we expect a low level of genetic diversity at mitochondrial markers and congruent geographic structures of *Wolbachia* and mitochondrial genomes. To address these questions, we evaluated the spatial genetic variation in 26 SBPH populations sampled from most of the species' range in China. To gain a reliable picture of genetic variation, we employed three different types of molecular markers: (i) 13 microsatellite loci that had previously been published[26] (6) or were presently identified from an expressed library (7); (ii) two mitochondrial DNA gene sequences (*COI* and *COII*); and (iii) the multilocus sequence typing of Baldo *et al.* (2006)[27] for the endosymbiotic bacterium *Wolbachia*.

Results

Genetic diversity. The concatenated mitochondrial sequences of the *COI* and *COII* genes were obtained from 1323 out of 1328 samples. In the concatenated sequence (1368 bp), 85 of the nucleotides (6.2%), were variable between the 1323 SBPH samples. Of the 85 variable sites, 39 were parsimony informative sites. No nuclear mitochondrial DNA sequences (numts) were identified after comparisons with the published complete mitochondrial genome[28] and examinations of sequence translation. Of the 1323 samples, 107 haplotypes were identified (Fig. 1B), of which 70 were unique haplotypes, five were shared within populations and 32 were shared between populations. Three haplotypes of high frequency accounted for 73.5% of the haplotypes. H1 was the most common haplotype, being present in 620 individuals distributed in all 26 populations. H10 was found in 225 individuals from 23 populations and H2 was found in 128 individuals from 24 populations.

Table 1 shows genetic diversity indices for each SBPH population sample. The populations showed moderately high haplotype diversity and low nucleotide diversity at mtDNA sequences. Overall haplotype diversity and nucleotide diversity were 0.739 and 0.18%, respectively. At microsatellite markers too, the SBPH populations showed a high level of genetic diversity. The allelic richness (A_R) based on a minimum population size of 23 diploid individuals ranged from 8.3 in DD10 to 10.1 in SH with an average value of 9.1 across populations. The unbiased expected heterozygosity (uH_E) values were quite high, ranging from 0.752 to 0.810 (Table 1, Supplementary Table S1 online). Details of single-locus indices of genetic diversity can be found in Supplementary Table S1.

Figure 2 shows the results of a comparison of genetic diversity between climatic zones. For the mitochondrial markers, both the levels of haplotype diversity (H_d) and the levels of nucleotide diversity (π) were significantly lower in the moderate temperate zone (MT) than in the three remaining climatic zones: WT (warm temperate zone), SS (southern subtropical zone) and NS (northern subtropical zone). For H_d, the P values were <0.001 for MT *vs.* WT and MT *vs.* NS, and $= 0.03$ for MT *vs.* SS. For π, the P values were <0.001 for MT *vs.* WT and MT *vs.* NS and $= 0.014$ for MT *vs.* SS. In addition, the levels of nucleotide diversity (π) were also significantly lower in SS than in WT ($P = 0.048$) and NS ($P = 0.020$). For the microsatellite markers, the only significance indicated that the levels of A_R were significantly higher in MT than in WT ($P = 0.024$).

Population structure. Pairwise F_{ST} values computed from mitochondrial DNA data ranged from -0.078 to 0.442, with an average F_{ST} of 0.075. Exact tests showed that 120 of the 325 pairwise populations were significantly different (Fig. 3A and Supplementary Table S2 online). Interestingly, 90 of the 120 significant pairwise differentiation levels were between populations from the MT zone and the populations from the three remaining climatic zones. The average F_{ST} value between populations from the MT zone and

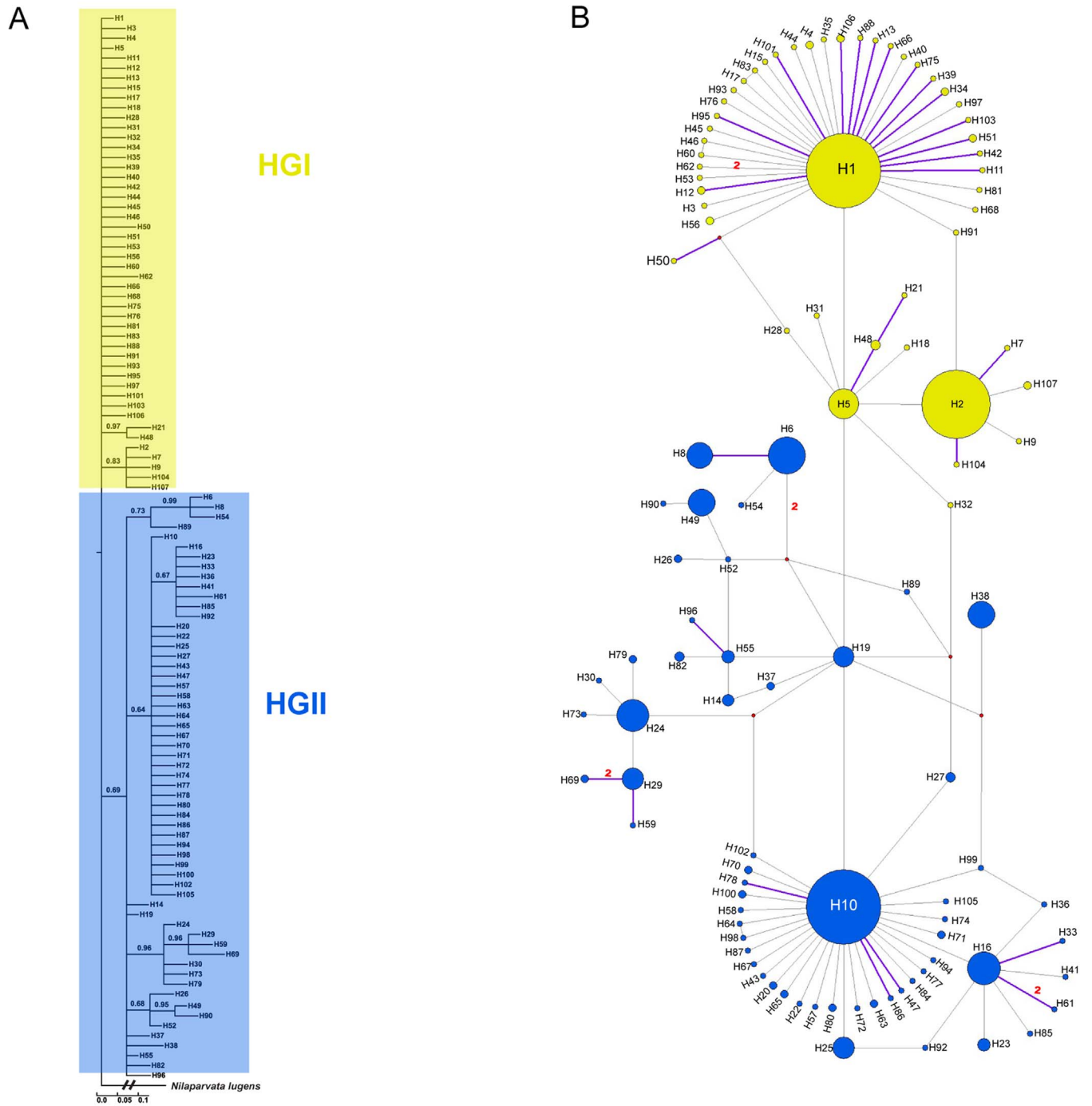

Figure 1 | Bayesian phylogeny (A) and Haplotype network (B) based on the concatenated sequences for the mitochondrial *COI* and *COII* genes (1 368 bp). (A) The branch of the out-group taxa *Nilaparvata lugens*, is truncated as indicated by slashes. Only posterior probability values > 0.5 are indicated at each node. The best fit model based on Bayesian Information Criterion (BIC) values was HKY+I. (B) The sizes of circles are proportional to the haplotype frequencies. Small red circles represent internal (unsampled) nodes. The number of mutations >1 is shown next to branches. Purple lines represent non-synonymous substitutions. HGI, mitochondrial DNA haplogroup I; HGII, mitochondrial DNA haplogroup II.

populations from the three remaining climatic zones was 0.176. In comparison, the F_{ST} values for other between-zone population pairs were very low, with an average F_{ST} of 0.016. The principal coordinate analysis (PCoA) also showed that the six populations from the MT zone (MDJ, HRB10, HRB12, SJ, YJ11 and YJ12) were separated from the other populations (Fig. 4A). A Bayesian inference (BI) phylogenetic tree and the haplotype network derived from 107 concatenated mtDNA sequences revealed two well-supported haplogroups (Fig. 1A and 1B). The mean P-distance between the two haplogroups was 0.4%. These haplogroups, named HGI and HGII, had non-random distributions across the sampling localities. In general, the frequency of HGI (61.3%) was higher than that of HGII (38.7%) over all the sampled populations, and had absolute dominance in the MT zone (95.1% in total, Fig. 5; 94.6% in females, and 97.9% in males, Supplementary Fig. S1A and 1B online).

Pairwise F_{ST} values computed over microsatellite loci were very low, ranging from −0.017 to 0.027, with an average F_{ST} of 0.006 (Fig. 3B and Supplementary Table S2 online). The standardized pairwise F_{ST} values ranged from −0.082 to 0.114, with an average F_{ST} of 0.027 (Fig. 3C and Supplementary Table S3 online). We did not

Table 1 | Locations and dates of the collection of small brown planthoppers in China and basic genetic diversity indices calculated with 13 microsatellites and the concatenated mitochondrial DNA sequences (*COI* and *COII*)

				Microsatellites				mtDNA		
Locality/zone	Pop code	Sampling dates	*N*	N_A	A_R	H_O	uH_E	N_h	H_d	π (%)
Mudanjiang/MT	MDJ	5-Jul-12	48♀ + 17♂/48♀ + 17♂	12.6	9.5	0.673	0.776	4	0.397	0.054
Harbin/MT	HRB10	27-Jul-10	46♀ + 0♂/48♀ + 0♂	10.5	9.0	0.609	0.779	4	0.268	0.040
Harbin/MT	HRB12	02-Jul-12	48♀ + 22♂/48♀ + 22♂	12.7	9.4	0.684	0.773	7	0.483	0.093
Shuangji/MT	SJ	26-Jul-10	46♀ + 5♂/46♀ + 4♂	11.3	9.2	0.665	0.790	9	0.627	0.104
Yanji/MT	YJ11	28-Aug-11	35♀ + 0♂/43♀ + 0♂	11.0	9.9	0.694	0.786	7	0.525	0.081
Yanji/MT	YJ12	10-Jul-12	48♀ + 5♂/47♀ + 5♂	12.1	9.4	0.668	0.778	10	0.633	0.131
Dandong/WT	DD10	24-Jul-10	48♀ + 0♂/48♀ + 0♂	9.8	8.3	0.662	0.772	13	0.867	0.171
Dandong/WT	DD12	16-Jul-12	46♀ + 5♂/46♀ + 6♂	10.8	8.8	0.689	0.765	15	0.808	0.188
Shenyang/WT	SY	23-Jul-10	48♀ + 0♂/48♀ + 0♂	11.0	9.0	0.684	0.768	13	0.699	0.183
Tangshan/WT	TS	20-Jul-10	48♀ + 23♂/47♀23♂	12.6	9.1	0.657	0.764	15	0.672	0.145
Dezhou/WT	DZ	22-Jun-12	48♀ + 11♂/48♀11♂	12.2	9.4	0.653	0.781	14	0.800	0.223
Jinan/WT	JNN	16-Jul-10	45♀ + 6♂/47♀ + 6♂	11.5	9.4	0.653	0.778	12	0.697	0.178
Jining/WT	JNG	13-Jul-10	44♀ + 11♂/47♀ + 11♂	11.2	9.0	0.668	0.783	12	0.751	0.189
Xinxiang/WT	XX	22-Jun-10	48♀ + 0♂/47♀ + 0♂	11.0	8.7	0.597	0.752	13	0.759	0.213
Xuzhou/WT	XZ	30-May-12	48♀ + 0♂/48♀ + 0♂	10.4	8.6	0.678	0.763	17	0.863	0.226
Xinyang/NS	XY	25-Jun-10	48♀ + 16♂/48♀ + 16♂	12.0	9.1	0.655	0.777	17	0.810	0.207
Yancheng/NS	YC	14-Jun-10	48♀ + 16♂/48♀ + 16♂	12.0	9.1	0.642	0.766	14	0.764	0.180
Hefei/NS	HF10	22-Jun-10	40♀ + 10♂/40♀ + 10♂	10.6	8.7	0.640	0.766	16	0.781	0.211
Hefei/NS	HF12	23-Jul-12	44♀ + 0♂/43♀ + 0♂	10.2	8.8	0.624	0.774	14	0.793	0.190
Nanjing/NS	NJ	10-Jun-10	48♀ + 22♂/48♀ + 22♂	12.2	9.4	0.638	0.783	20	0.663	0.163
Shanghai/NS	SH	25-Jun-10	46♀ + 0♂/45♀ + 0♂	12.5	10.1	0.690	0.808	14	0.808	0.196
Hangzhou/NS	HZ	23-Jun-10	47♀ + 9♂/47♀ + 9♂	11.6	9.1	0.651	0.773	17	0.808	0.202
Longyan/SS	LY	27-May-10	35♀ + 0♂/35♀ + 0♂	10.4	9.3	0.732	0.789	10	0.714	0.190
Yongfu/SS	YF	20-May-10	23♀ + 0♂/22♀ + 0♂	9.0	9.0	0.699	0.757	7	0.762	0.134
Nanning/SS	NN	02-Jun-10	5♀ + 0♂/6♀ + 0♂	5.4	-	0.774	0.810	4	0.800	0.146
Guangzhou/SS	GZ	11-Jun-10	47♀ + 10♂/47♀ + 10♂	10.3	8.4	0.674	0.766	10	0.630	0.149

MT, moderate temperate zone; WT, warm temperate zone; NS, northern subtropical zone; and SS, southern subtropical zone; $N_♀$, sample sizes of females subjected to microsatellite DNA/mtDNA examination; $N_♂$, sample sizes of males subjected to mtDNA examination only; N_A, number of alleles per locus; A_R, allelic richness; H_O, observed heterozygosity; uH_E, unbiased expected heterozygosity; N_h, number of haplotypes; H_d, haplotype diversity; π, nucleotide diversity.

detect significant genotypic differentiation between any pairwise populations by using exact tests. For the principal coordinate analysis (PCoA), all of the populations except TS showed little genetic structure (Fig. 4B), though the pairwise F_{ST} values between TS and the other populations were very low (0.002~0.027, Fig. 3B, Supplementary Table S2 online). Accordingly, STRUCTURE[29] analyses suggested that SBPH most likely forms a single genetic cluster. Indeed, for K = 1, the log-likelihood of the multilocus genotypic data was maximal and had low variance (see Supplementary Fig. S2 online).

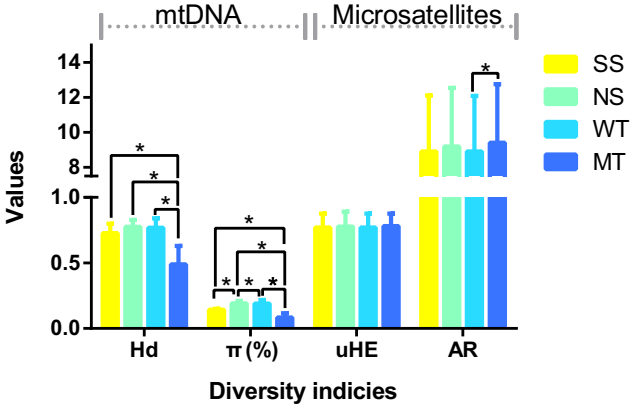

Figure 2 | Comparison of genetic diversity between four climatic zones in China. MT, moderate temperate zone; WT, warm temperate zone; NS, northern subtropical zone; and SS, southern subtropical zone. H_d, haplotype diversity; π, nucleotide diversity; A_R, allelic richness; uH_E, unbiased expected heterozygosity. * Indicates $P < 0.05$.

Geographic and environmental associations. In our microsatellite data set, no isolation by distance (IBD) effects were detected with the standardized pairwise F_{ST} (Z = 17.184, r = −0.071, P = 0.735; Fig. 6A). By contrast, there was a significant IBD effect across the 22 geographic populations in the mtDNA sequence data (Z = 65.357, r = 0.383, P = 0.001; Fig. 6B). When the populations from the MT zone were excluded, we were no longer able to detect the IBD effect across the remaining 16 populations (Z = 7.794, r = −0.093, P = 0.778).

The logistic regression analyses by SAM software indicated that the distributions of the two mtDNA haplogroups were significantly associated with the first two PCA axes ($P < 0.001$). PC1 and PC2 axes accounted for 71.1% and 13.4% of the climatic variation across the sampling sites. Supplementary Table S4 shows that PC1 was primarily related to the mean (or maximum) of temperatures while PC2 mostly explained the amount of precipitation and climate variability (seasonality of precipitation and isothermality). The values of mean (and maximum) temperatures, isothermality, annual precipitation, seasonality of precipitation and annual relative humidity for each sampling location are presented in Supplementary Table S5. Further, partial Mantel tests showed that HGI frequencies were significantly correlated with PC1 (r = 0.437, $P < 0.001$) but not with PC2 (r = −0.055, P = 0.300). When the IBD effect was removed, the significant correlation between the HGI frequencies and PC1 was still detected (r = 0.237, $P < 0.05$).

Demographic history. For neutrality tests, significantly negative Tajima's D values (−2.127, $P < 0.001$) and Fu's F_S (−26.018, $P < 0.001$) were found over all populations. The mismatch distribution over all populations was deemed unimodal and failed to reject the hypothesis of a sudden expansion because of the small, non-significant Harpending's raggedness (HR) index (0.063, P = 0.294,

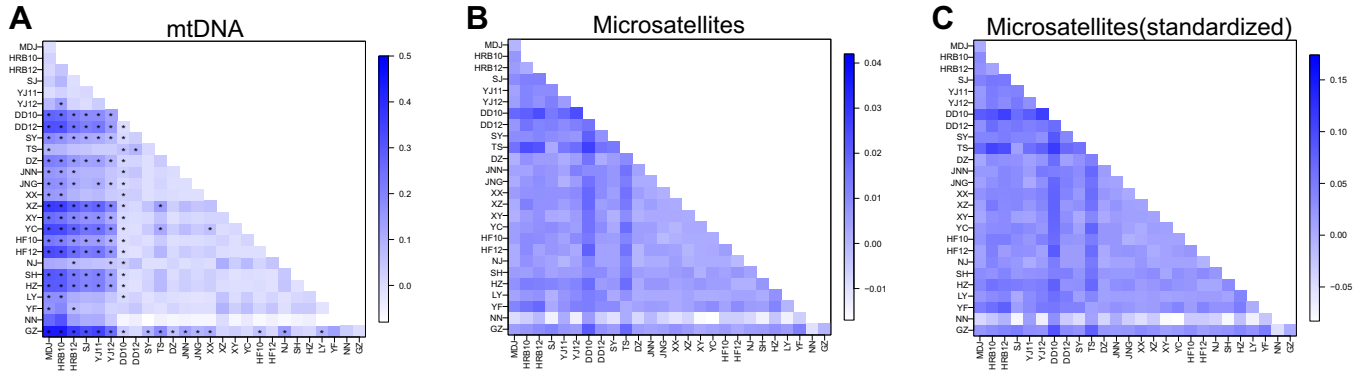

Figure 3 | Heatmap of pairwise F_{ST} values estimated from mitochondrial DNA sequence data (A), microsatellite data (B) and standardized pairwise F_{ST} for microsatellite data (C) between all populations. *indicates significant difference after Bonferroni correction ($P < 0.000154$). Populations are ordinated by climatic regions: MT, WT, NS and SS. See Fig. 5 for population geolocalization.

Fig. 7A). A Bayesian skyline plot (BSP) revealed a relatively explicit demographic history for population expansion by showing that the SBPH population underwent a sharp demographic expansion (~100 to 1000 fold) (Fig. 7B).

Wolbachia detection and multilocus sequence typing (MLST). In total, we screened 1328 SBPH individuals across the sampled 26 populations for *Wolbachia* infection. Surprisingly, all individuals were infected. MLST genotyping of 398 representative *Wolbachia*-positive individuals (including 210 females and 188 males) showed that the sequences of each of the five genes selected for the MLST analysis (*gatB*, *coxA*, *hcpA*, *ftsZ*, and *fbpA*) were identical. By comparing with a *Wolbachia* MLST database (http://pubmlst.org/wolbachia/), the sequence type (ST) number ST213 was obtained, which was consistent with our previous study[30].

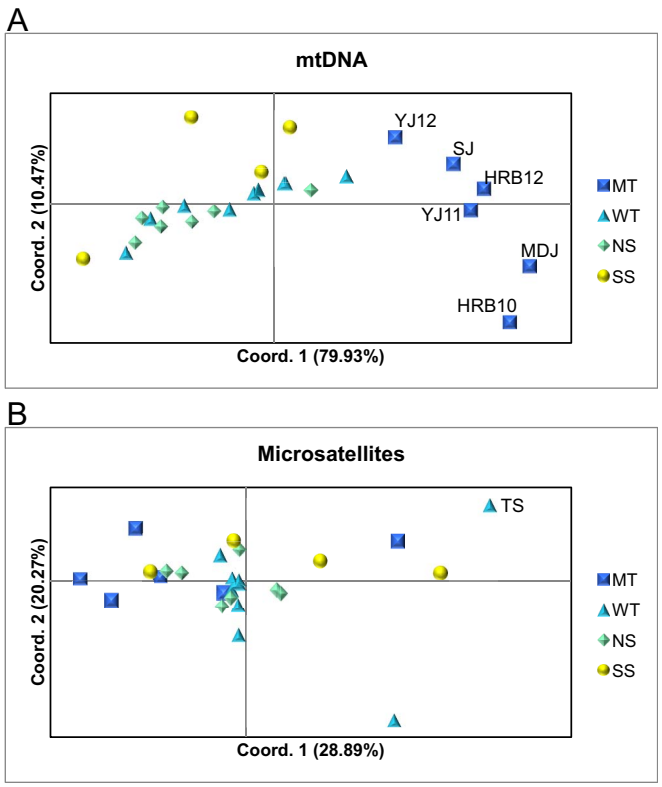

Figure 4 | Principal coordinates analysis based on pairwise F_{ST} values for mitochondrial DNA data (A) and the standardized pairwise F_{ST} values for microsatellite data (B).

Discussion

The effect of Wolbachia on host evolution. The cotransmission of *Wolbachia* and mitochondria is expected to cause the bacteria to have an indirect impact on mitochondrial DNA diversity, as a result of a selective sweep of the mito-type associated with the infection[21,22]. In this study, all individuals were infected with the same or at least very closely related *Wolbachia* strains. This compares to an average infection frequency of 91.7% reported for SBPH populations in China and Vietnam[30] and an average infection frequency of 65.9% for SBPH populations in Japan[19]. The rapid growth in the infection frequencies of the same or at least very closely related *Wolbachia* strains indicates a recent invasion of this endosymbiont in SBPH. Since these strains can induce strong cytoplasmic incompatibility (CI) in SBPH[9,19,20], limited mtDNA diversity would have been expected. However, haplotype diversity was moderately high (0.739), suggesting no or little effect of *Wolbachia* on mtDNA diversity. The observation that different mtDNA haplotypes carry the same or very closely-related *Wolbachia* strains strongly indicates horizontal transmissions of *Wolbachia* between SBPH individuals. A similar phenomenon has also been reported in the fire ant *Solenopsis invicta*[31] and the fruit fly *Drosophila willistoni*[32]. The horizontal transmissions of *Wolbachia* make the natural infection status unstable in SBPH populations, and also interrupt the host speciation process induced by CI. Our data suggest that *Wolbachia* alone may not be sufficient to promote population divergence and speciation of the host over long periods of evolutionary time.

Dispersal pattern of SBPH. In agreement with Ji et al. (2010)[13], the SBPH populations in China were found to show a high degree of genetic connectivity, despite a high level of polymorphism at the two types of molecular markers. This population structure pattern is consistent with those of other migratory insects that are characterized by genetic homogeneity between populations separated by large geographic distances[16,18,33–35]. The population genetic structure of SBPH in China contrasts with the strong population genetic structure of other insects that are widely distributed, but which have limited dispersal ability, such as the striped riceborer *Chilo suppressalis* (Walker)[36].

Several lines of evidence support the high dispersal ability of SBPH. First, our microsatellite results from pairwise F_{ST}, PCoA and Bayesian clustering analyses indicated a lack of geographic structure among populations. The PCoA result of mitochondrial DNA also showed that all of the populations were similar except those from the MT zone (i.e, MDJ, HRB10, HRB12, SJ, YJ11, and YJ12; and see below). In addition, there was no obvious evidence for isolation by distance (IBD). Usually, IBD effects are pronounced in moderately mobile species but weak in both low-mobility and high-mobility

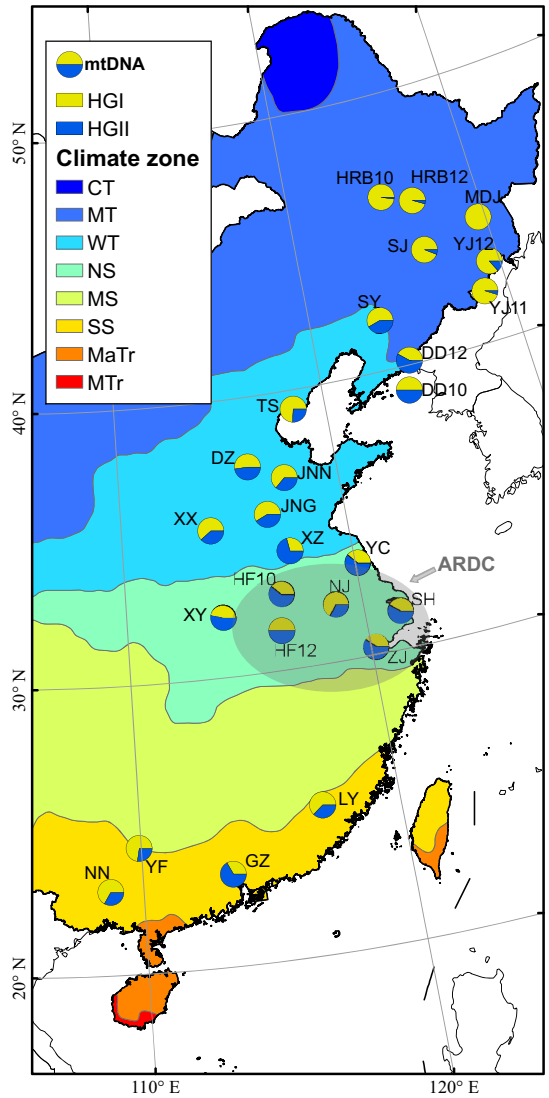

Figure 5 | Sampling locality and the distributions of mitochondrial DNA haplogroups of the SBPH populations. CT, cold temperate zone; MT, moderate temperate zone; WT, warm temperate zone; NS, northern subtropical zone; MS, middle subtropical zone; SS, southern subtropical zone. MaTr, marginal tropical zone; MTr, middle tropical zone; ARDC, ancient rice domestication center; HGI, mitochondrial DNA haplogroup I; HGII, mitochondrial DNA haplogroup II (The map is made by ArcGIS 10.2 software, http://www.arcgis.com/features/).

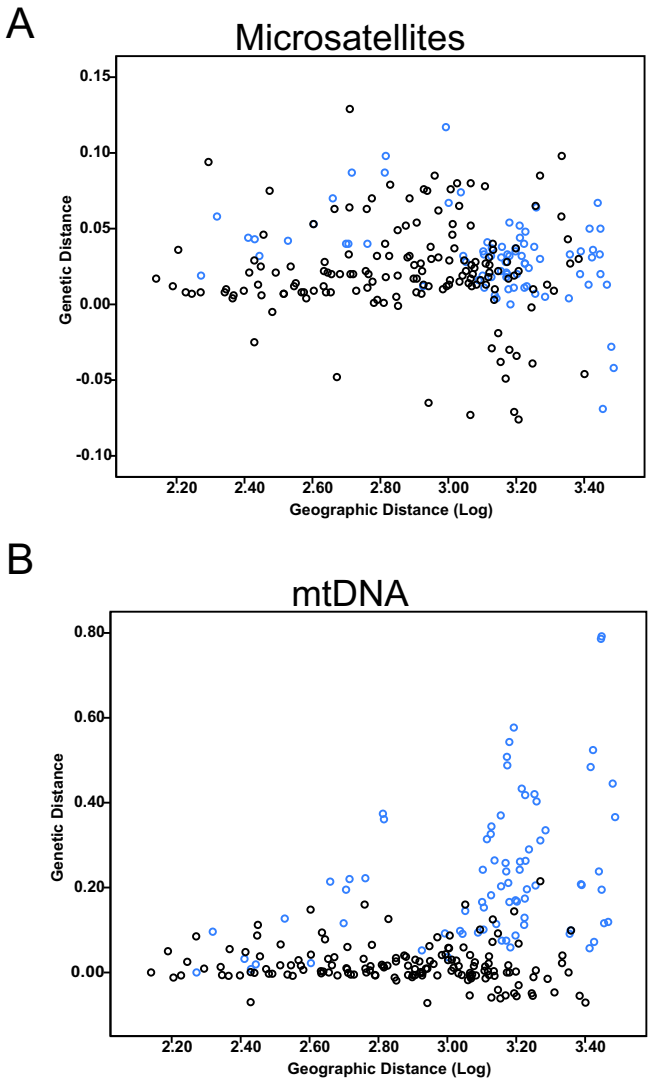

Figure 6 | Scatter plots of genetic distance ($F_{ST}/1 - F_{ST}$) vs. geographic distance for pairwise population comparisons based on microsatellite (A) or mtDNA data (B). Blue circles represent the comparisons associated with populations from moderate temperate zone (MT).

species, since extensive gene flow homogenizes populations across large geographic areas[37].

Furthermore, the SBPH populations in China possess high levels of mtDNA haplotype diversity with low levels of nucleotide diversity. This diversity combination has been considered to be mostly the result of demographic expansion after a period of small effective population size, retaining new mutations[38]. SBPH populations appear to have experienced a recent demographic expansion, and this conclusion was supported by both mismatch and BSP analyses in our study. However, this diversity combination type may also reflect a high level of dispersal in SBPH since it allows for the sweeping away of deleterious mutations that had built up within isolated populations[39]. This is why the combination of high levels of haplotype diversity with low levels of nucleotide diversity at mtDNA level is frequently observed in species with a high migration rate[18,40].

The low level of structure observed among populations suggests that outbreak occurrences of SBPH and RSV may not only depend on local recruitment but also on immigration. However, the lack of genetic differentiation prevented us from quantifying migration rates between populations and the frequency of long-distance migration events. Although assignment tests based on multilocus genotype data can help to estimate recent migrations, the accuracy largely depends on the degree of genetic differentiation between populations[41,42]. Computer simulations have also shown that as the dispersal rate increases, and genetic differentiation decreases, the ability to distinguish the source of an individual also falls[43]. The lack of population differentiation between SBPH populations makes this analysis impractical.

Discordance between mitochondrial DNA and nuclear microsatellites. The mtDNA haplotypes had a non-random distribution across the sampling localities in the face of gene flow (Fig. 5 and Supplementary Fig. S1 online). The levels of mitochondrial diversity were significantly lower in the MT zone than in other climatic zones. Conversely, the level of microsatellite diversity was generally similar across climatic zones (Fig. 2). Mitochondrial HGI had a high frequency in the MT zone, and had temporal stability (Fig. 5 and Supplementary Fig. S1 online). The PCoA result for mtDNA also showed that the six population samples from the MT

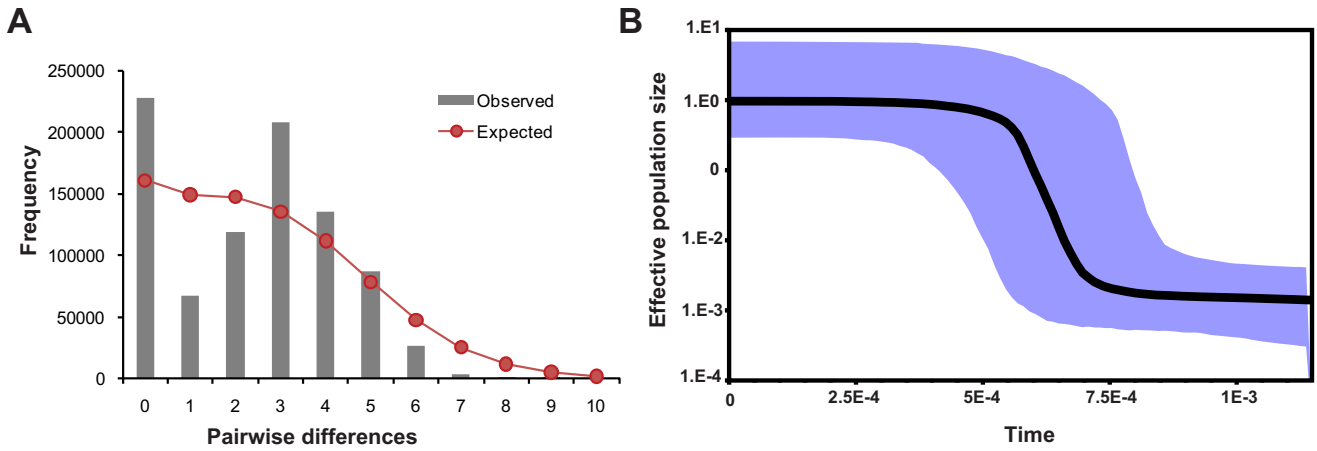

Figure 7 | Mismatch distributions (A) and Bayesian skyline plots (B). (B) Dark lines represent mean inferred effective population size (*Nef*) multiplied by the generation time (T) in years, blue areas mark the 95% highest probability density (HPD) intervals. *Nef* × *T* is presented on a logarithmic scale.

zone (MDJ, HRB10, HRB12, SJ, YJ11 and YJ12) were genetically different from the other populations. However, the microsatellite data revealed a lack of genetic structure in China (Fig. 4). The lower differentiation levels at microsatellites remained even after standardization (Fig. 3C, Supplementary Table S3 online). So why is there such a large haplotype skew over nuclear data in the MT zone for SBPH? The biogeography of mitochondrial and nuclear discordance in animals has been well reviewed and meta-analyzed by Toews and Brelsford (2012)[44]. Mito-nuclear discordance arising in the face of strong gene flow has rarely been reported. Usually, mitochondrial introgression from a close species, male-biased dispersal, demographic expansion or selection on mtDNA are considered as the main reasons for this mito-nuclear discordance[45–49].

In our data and literature, there was no evidence for hybridization of SBPH with a recently formed species or divergent population, and the divergence between the two mitochondrial haplogroups was low (*P*-distance = 0.4%). There was no evidence for a contribution of male-biased dispersal to mito-nuclear discordance either. Male-biased dispersal is common in nature, and unlike males, macropterous females of SBPH can decrease in number with low population density[50]. This suggests higher or longer-distance dispersal in males, at least when the population density is low, but under such a hypothesis, the prevalence of HGII should be expected to be higher in the male than in the female populations from the MT zone. Similar patterns of distribution of the two haplogroups for both genders do not support the male-biased dispersal hypothesis in this species. This is probably explained by the same high rate and long distance of dispersal for females as for males when the population density is high. When population sizes are large, the resulting large number of migrants prevails in affecting population genetic differentiation.

An alternative scenario would be that SBPH has experienced a recent northward colonization associated with genetic drift effects. Structuring effects in the northeastern region (i.e. MT zone) would be expected to have a more pronounced impact in the mitochondrial genome than the nuclear genome, since mtDNA is haploid and maternally inherited, and therefore has a fourfold smaller effective population size. The lower mtDNA diversity and significant differentiation in the MT zone are congruent with this scenario. The reason for northward expansion is unclear here. However, some consideration should be given to the history of rice domestication since, although polyphagous, SBPH mainly occurs on this host plant. According to archaeological evidence, the eastern region (NS zone) of China is one of the rice domestication centers (Fig. 5)[51], and, 5700 ~ 3000 years ago, the cultivation area expanded in the northern and southern regions of China[52]. Rice cultivation in the northeastern region (MT zone) started more recently, around the end of the 19th century. The expansion of rice growing areas may have provided suitable food sources for the SBPH populations, and subsequently triggered a range expansion northward and southward from the eastern center.

A final alternative explanation is local adaptation of mitochondrial haplogroups to different climates. The finding that the mitochondrial HGI frequencies were significantly correlated with the first PCA axis (even when the IBD effect was removed) may indicate that temperature plays an important role in shaping the distributions of mitochondrial haplogroups. Considering the low winter temperatures in the MT zone (the mean winter temperatures of the four sampling sites in the MT zone range from −17.1 to −12.0°C), the enrichment of HGI in the MT zone may indicate that the HGI mitochondrial haplotype (or another allele at another locus it is linked with) is more favored under cold climates than the HGII mitochondrial haplotype. Mitochondria not only provide most of the energy (ATP) in animal cells through oxidative phosphorylation (OXPHOS), but also provide heat to maintain body temperature through proton leakage[53]. Certain mitochondrial lineages (or haplogroups) characterized by reduced coupling efficiency of OXPHOS and increased efficiency of proton leakage have been suggested to adapt to colder climates, resulting in their enrichment in such climates[54–56]. Although we did not find any non-synonymous mutations at the two studied cytochrome oxidase genes, we cannot rule out the probability that their genetic variation is impacted by selection acting on the remaining 11 mitochondrial protein-coding genes through genetic hitchhiking. Further studies are needed to identify the candidate genes for cold adaptation by whole-genome comparisons and functional assays of the two types of mitochondria.

The traditional view that sequence variation in the mtDNA genome is selectively neutral is being challenged by a growing body of evidence for natural selection on mitochondrial genes[54–56]. Recently, Kazancıoğlu & Arnqvist also documented negative frequency-dependent selection (NFDS) on mtDNA haplotypes in laboratory populations of the seed beetle (*Callosobruchus maculates*)[57]. Whether the maintenance of the mtDNA diversity and the distribution of the mtDNA variations in SBPH populations are associated with NFDS, or the combined effect of NFDS and climate adaptation need to be studied in the future.

Methods

Sample collection and DNA extraction. The study area consisted of 22 sampling locations along a gradient covering four climatic zones (moderate temperate zone, MT; warm-temperate zone, WT; northern subtropical zone, NS; and southern subtropical zone, SS) in China[58]. SBPH adults were sampled from rice plants at 22 sites during the summers (May to August) of 2010, 2011 and 2012. Four sites (Harbin, Yanji, Dandong and Hefei) were sampled twice in two years (Table 1, Fig. 5). The

geographic distances between sampling sites varied from 138 to 3071 km. To avoid sampling siblings, we collected only one SBPH per host plant and selected host plants that were at least 1 m apart. The samples were immediately preserved in absolute ethanol and then stored at −20°C in the laboratory until DNA extraction. In all, 1140 adult females were collected, with sample sizes ranging from 6 to 48 per population. In contrast, only 188 adult males were collected from 15 of the 22 sites (Table 1). Total genomic DNA was isolated from the combined head and thorax of each individual using a modified CTAB method.

Climate GIS layers for the study area were downloaded from the online WORLDCLIM database (www.worldclim.org). The BIOCLIM algorithm implemented in DIVA-GIS software was used to derive 19 climatic variables for 21 of the 22 sampling sites (except for NN) from three input parameters (mean monthly values of maximum temperature, minimum temperature, and precipitation). Because many of these climatic variables were likely to be correlated, we used SPSS 17.0 to perform a principal component analysis (PCA) on a correlation matrix of the 19 climatic variables.

Mitochondrial DNA sequencing. Portions of the *COI* gene (895 bp) and *COII* gene (650 bp) of mtDNA were separately amplified by PCR for all samples. The primer pair for the *COI* gene (F: 5′-TCTCATTACATATCGCTGGAGTTAG-3′; R: 5′-GTAGTCTGAATATCGTCGTGGTATT-3′) was designed from the published complete mitochondrial genome of SBPH[28] using Primer premier 5.0 software (http://www.premierbiosoft.com). The *COII* gene fragment was amplified with primers *COII-1* and *COII-2*[13]. PCR was performed in a Veriti Thermal Cycler (ABI Biosystems). All PCR reactions consisted of 40 μl reaction volumes containing 10–100 ng template DNA, 0.2 μl of DreamTaq polymerase (5 U/μl), 4.0 μl 10×DreamTaq Buffer (including 20 mM $MgCl_2$; Fermentas), 4 μl dNTPs (2.0 mM each, Fermentas, Canada), 1 μl each of the primers (20 μM) and autoclaved distilled water to volume. The thermal profile used an initial denaturation step of 95°C for 3 min followed by 35 cycles of denaturing at 94°C for 30 s, annealing at 55°C for 30 s, and extension at 72°C for 1 min. A 15 min final extension at 72°C was added at the end of the cycle. Negative controls were included in both DNA isolation and PCR reactions. After verification by gel electrophoresis, the PCR templates were purified and then sequenced in both directions using the same primer pairs on an Applied Biosystems 3130 Genetic Analyzer.

Microsatellite development, genotyping and null alleles. New microsatellites were isolated from the expressed sequence tags of SBPH, which were downloaded from the Short Read Archive of the National Center for Biotechnology Information (NCBI) with accession numbers *SRX016333* and *SRX016334*. Data mining and experimental procedures were done according to Sun *et al.* (2011)[59]. Seven new microsatellites were developed and proved to be highly polymorphic, with 7 to 26 alleles per locus (see Supplementary Table S6 for primer sequences, repeat motifs and size ranges). These new microsatellites, together with six compound microsatellite loci developed previously by Sun *et al.* (2012)[26], were genotyped. Each of the 13 loci was amplified in a single tube separately for each individual. PCR for the seven newly developed microsatellites was performed according to Sun *et al.* (2011)[59]. PCR for the six previously developed microsatellites was performed according to Sun *et al.* (2012)[26]. Products were genotyped on an Applied Biosystems 3130 Genetic Analyzer.

No linkage disequilibrium between loci was detected. A large excess of significant departures from *HWE* was observed in 130 of the 338 single-locus exact tests after false discovery rate (FDR) correction[60]. Five loci (*LS1*, *LS3, LS4, LS5* and *LS6*) accounted for 107 of the significant outcomes. Null allele analysis by Micro-Checker software (Ver. 2.2.3) revealed that the departure from *HWE* was almost entirely due to heterozygote deficiency. Only two cases (locus *LS11* in SJ and LY) were caused by heterozygote excess (see Supplementary Table S1 for more details). As null alleles may inflate genetic differentiation[61], all of the population structure analyses below were conducted separately on two data sets: the original data set of 13 loci and a reduced data set of eight loci (i.e., excluding *LS1* and *LS3* ~ *LS6* with high null allele frequencies). Since highly congruent results were obtained in these analyses, we only present the results obtained with the original data set.

Screening for Wolbachia and multilocus sequence typing (MLST). We first checked for the presence of *Wolbachia* infection in all 1328 samples, by using PCR primers *wsp*81F and *wsp*691R[62]. PCR was performed according to Zhang *et al.* (2013)[30] and 13 individuals were tested twice to assess repeatability. All amplifications, including positive and negative controls, were checked on a 1% agarose gel. We then selected all males and 12 *Wolbachia*-positive females from each population sampled in 2010 (except for NN, only 6 individuals in this population) for MLST (398 individuals in total). The sequences of the MLST genes (*gatB*, *coxA*, *hcpA*, *ftsZ*, and *fbpA*) were amplified with standard primers and protocols (Baldo *et al.* 2006)[27]. After verification by gel electrophoresis, the PCR templates were purified, then sequenced in both directions using the five primer pairs respectively on an Applied Biosystems 3130 Genetic Analyzer.

mtDNA sequence analyses. DNA sequences were assembled and aligned with Codoncode Aligner 3.6.1 (CodonCode, Dedham, MA, USA), and manually edited before creating consensus sequences. To eliminate missing data, all sequences of the *COI* and *COII* genes were truncated to the same length of 769 bp and 599 bp, respectively, and the truncated sequences of the two genes were then concatenated into a data matrix for subsequent analysis. In order to assess the genetic variation within populations, the number of haplotypes (N_h), nucleotide diversity (π), and haplotype diversity (H_d) were calculated with DNASP v5.10.01. Shapiro-Wilk tests implemented in R software indicated that distributions of *H*d and π from each respective climatic zone (SS, NS, WT and MT) were normal. *T*-tests were thus used to evaluate the significance of differences in diversity estimates H_d and π of the female populations between the four climatic zones and the *P* values were corrected by the FDR correction method.

The degree of population differentiation was quantified using pairwise F_{ST} values in Arlequin 3.5. Genotypic differentiation between pairwise populations was detected by an exact test. In order to visualize these genetic relationships between populations, the pairwise F_{ST} matrix was then used to construct a principal coordinates analysis (PCoA) in GenAlEx 6.5. To detect an isolation-by-distance (IBD) effect, we compared the $F_{ST}/(1 - F_{ST})$ matrix with a geographic distance matrix (Log Km) using the Mantel test implemented in IBDWS 3.16, with significance tests performed over 10^3 permutations. The geographic distances between sampling sites were computed based on the GPS coordinates. For the four sites that were sampled twice, we used only the first year of collection. A Reduced Major Axis (RMA) regression was used to estimate the slope and intercept of the isolation-by-distance relationship. The genealogical relatedness between haplotypes was represented first through a median-joining network constructed with Network 4.6, and the phylogenetic relationships between haplotypes were also inferred by Bayesian inference (BI) using MrBayes 3.1.2. *N. lugens* was added as an outgroup (GenBank Accession No. JX880069). The best fit model of nucleotide substitution was determined based on the Bayesian Information Criterion (BIC) calculated by jModelTest 2.1.2. The Markov chain was run for 10 million iterations using four chains with a sampling period of 100 generations, and we discarded the initial 20% as burn-in. As we found that the 107 haplotypes were divided into two haplogroups, we calculated the mean P-distance between the two haplogroups using MEGA 5 software.

Demographic history was explored taking three different approaches. First, Tajima's *D*[63] and Fu's F_S[64] were used to test for neutrality. Second, the mismatch distribution of pairwise sequences was calculated to identify the demographic history, which was characterized by the mismatch distribution modal and Harpending's raggedness index[65]. Both the neutrality test and mismatch distribution analysis were conducted in Arlequin 3.5 with 10^4 simulated samples. Finally, a Bayesian skyline plot (BSP) analysis was performed with BEAST v1.7.5. We adopted the piecewise-linear skyline model and 10 groups for Bayesian skyline coalescent tree priors. The MCMC chains were run with 10^8 iterations, sampling every 10^3 iterations and discarding the initial 20% as burn-in. The relaxed clock with uncorrelated lognormal distribution was used, which allowed rate variation between branches. Default values were used for all other parameters. The convergence of the chain was checked by the T_{RACER} v1.5 program (http://tree.bio.ed.ac.uk/software/tracer) to ensure that effective sample sizes were above 200.

As we observed a non-random distribution of the two mtDNA haplogroups, we tested for an association between haplogroup frequencies and climatic variables (PC1 and PC2) using logistic regressions. We first carried out two univariate logistic regressions to test for associations between the frequencies of the two mitochondrial haplogroups and the environmental variable PC1 using the SAM program. We considered a correlation as significant only when two logistic regression tests (LRTs, G and Wald tests) rejected the null hypothesis of no association between the genetic and the environmental variables (at the 0.1% level) after FDR correction. Partial Mantel tests were then performed in ZT software to evaluate the specific contribution of PC1 or PC2 to the distribution of mtDNA haplogroups. This complementary approach made it possible to evaluate the effect of PC1 on the distribution of mtDNA haplogroups by removing the PC2 effect, and vice versa. In order to remove the IBD effect, we also performed partial Mantel tests between mtDNA haplogroup frequencies and PC1 or PC2 while controlling effects for geographic distances (Log Km). The Euclidean distance metrics of haplogroup I (HGI) frequencies and environmental variables (PC1 and PC2) were calculated by 'ecodist' implemented in R 3.0.1.

Microsatellite data analyses. The population genetic diversity indices, such as the number of alleles (N_A), observed heterozygosity (H_O), and unbiased expected heterozygosity (uH_E) were assessed using GenAlEx 6.5. Allelic richness (A_R) was calculated with FSTAT 2.9.3.2 using a rarefaction index (2N = 46) to account for different sample sizes, and the NN population was excluded owing to its small population size. In addition, we used Wilcoxon signed-rank tests applied on the 13 single locus values of the uH_E and A_R averaged over all populations of the four climatic zones to determine whether genetic diversity within populations differed significantly between climatic zones and the *P* values were corrected by the FDR correction method.

Pairwise F_{ST} values were calculated in Arlequin v3.5. Genotypic differentiation between pairwise populations was detected by an exact test. The microsatellite loci employed in this study had very high within-population heterozygosity, which tends to provide low estimates of F_{ST}. To obtain a more objective estimate of population differentiation[66], we calculated the standardized F_{ST}[67]. The standardized pairwise F_{ST} values were subsequently used for principal coordinate and IBD analyses. We used the individual clustering approach implemented in Structure v2.3.4 software to infer the number of functional population units. Simulations were run using the admixture ancestry model and the option of correlated allele frequency between populations. As our sampling scheme involved the collection of individuals from discrete distant locations, we used the USEPOPINFO option to incorporate sampling locations as prior information (LOCPRIOR)[68]. We set the number of genetic clusters from K = 1–12, because lnP(D) values always decreased when approaching K = 12 (see

Supplementary Fig. S2). The Markov chain Monte Carlo simulation was run 10 times for each value of K for 10^6 iterations after a burn-in period of 10^5. Leveled off alpha plots indicated the burn-in time was sufficient to achieve convergence between chains.

1. Broquet, T. & Petit, E. J. Molecular estimation of dispersal for ecology and population genetics. *Annu. Rev. Ecol. Evol. Syst.* **40**, 193–216 (2009).
2. Kokko, H. & López-Sepulcre, A. From individual dispersal to species ranges: perspectives for a changing world. *Science* **313**, 789–791 (2006).
3. Turelli, M., Barton, N. H. & Coyne, J. A. Theory and speciation. *Trends Ecol. Evol.* **16**, 330–343 (2001).
4. Osborne, J. L., Loxdale, H. D. & Woiwod, I. P. [Monitoring insect dispersal: methods and approaches.] *Dispersal Ecology* [Bullock, J. M., Kenward, R. E. & Hails, R. S. (ed.)] [24–49] (Blackwell, Oxford, 2002).
5. Kisimoto, R. Genetic variation in the ability of a planthopper vector *Laodelphax striatellus* (Fallén) to acquire the rice stripe virus. *Virology* **32**, 144–152 (1967).
6. Wei, T. Y. *et al*. Genetic diversity and population structure of rice stripe virus in China. *J. Gen. Virol.* **90**, 1025–34 (2009).
7. Li, J. C., Li, G. Z., Gao, L. Q. & Li, Q. S. Research on the occurance of *Laodelphgax striatellus* (Fallén). *Beijing Agric. Sci.* **16**, 24–27 (1998).
8. Kisimoto, R. Flexible diapause response to photoperiod of a laboratory selected line in the small brown planthopper, *Laodelphax striatellus* Fallén. *Appl. Entomol. Zool.* **24**, 157–159 (1989).
9. Hoshizaki, S. Allozyme polymorphism and geographic variation in the small brown planthopper, *Laodelphax striatellus* (Homoptera: Delphacidae). *Biochem. Genet.* **35**, 383–393 (1997).
10. Hirao, J. & Ito, K. Observations on rice planthoppers collected over the East China Sea in June and July 1974. *Jpn. J. Appl. Entomol. Zool.* **24**, 121–124 (1980).
11. Liu, H. G., Liu, Z. J. & Zhu, W. H. Results of net-trapping of brown planthoppers on China seas. *Acta Entomol. Sin.* **26**, 109–113 (1983).
12. Otuka, A. *et al*. The 2008 overseas mass migration of the small brown planthopper, *Laodelphax striatellus*, and subsequent outbreak of rice stripe disease in western Japan. *Appl. Entomol. Zool.* **45**, 259–266 (2010).
13. Ji, Y. H., Shi, W. Q., Le, W. J., Liu, L. & Zhou, Y. J. Sequencing and phylogenetic analysis of *CoII* gene in different populations of *Laodelphax striatellus*. *Jiangsu Agric. Sci.* **26**, 499–502 (2010).
14. Loxdalel, H. D. & Lushai, G. [Use of genetic diversity in movement studies of flying insects.] *Insect Movement: Mechanisms and Consequences* [Woiwod, I. P., Reynolds, D. R. & Thomas, C. D. (ed.)] [361–386] (CABI, London, 2001).
15. Chapuis, M. P. *et al*. Challenges to assessing connectivity between massive populations of the Australian plague locust. *Proc. R. Soc. B* **278**, 3152–60 (2011).
16. Endersby, N., McKechnie, S., Ridland, P. & Weeks, A. Microsatellites reveal a lack of structure in Australian populations of the diamondback moth, *Plutella xylostella* (L.). *Mol. Ecol.* **15**, 107–118 (2006).
17. Llewellyn, K. *et al*. Migration and genetic structure of the grain aphid (*Sitobion avenae*) in Britain related to climate and clonal fluctuation as revealed using microsatellites. *Mol. Ecol.* **12**, 21–34 (2003).
18. Wei, S. J. *et al*. Genetic Structure and Demographic History Reveal Migration of the Diamondback Moth *Plutella xylostella* (Lepidoptera: Plutellidae) from the Southern to Northern Regions of China. *PLoS ONE* **8**, e59654 (2013).
19. Hoshizaki, S. & Shimada, T. PCR-based detection of *Wolbachia*, cytoplasmic incompatibility microorganisms, infected in natural populations of *Laodelphax striatellus* (Homoptera: Delphacidae) in central Japan: has the distribution of *Wolbachia* spread recently? *Insect. Mol. Biol.* **4**, 237–243 (1995).
20. Noda, H., Koizumi, Y., Zhang, Q. & Deng, K. Infection density of *Wolbachia* and incompatibility level in two planthopper species, *Laodelphax striatellus* and *Sogatella furcifera*. *Insect Biochem. Mol. Biol.* **31**, 727–737 (2001).
21. Galtier, N., Nabholz, B., Glémin, S. & Hurst, G. Mitochondrial DNA as a marker of molecular diversity: a reappraisal. *Mol. Ecol.* **18**, 4541–4550 (2009).
22. Hurst, G. D. & Jiggins, F. M. Problems with mitochondrial DNA as a marker in population, phylogeographic and phylogenetic studies: the effects of inherited symbionts. *Proc. R. Soc. B* **272**, 1525–34 (2005).
23. Telschow, A., Flor, M., Kobayashi, Y., Hammerstein, P. & Werren, J. H. *Wolbachia*-induced unidirectional cytoplasmic incompatibility and speciation: mainland-island model. *PLoS ONE* **2**, e701 (2007).
24. Bordenstein, S. R., O'Hara, F. P. & Werren, J. H. *Wolbachia*-induced incompatibility precedes other hybrid incompatibilities in *Nasonia*. *Nature* **409**, 707–710 (2001).
25. Hurst, G. D. & Schilthuizen, M. Selfish genetic elements and speciation. *Heredity* **80**, 2–8 (1998).
26. Sun, J. T., Li, J. B., Yang, X. M. & Hong, X. Y. Development and characterization of nine polymorphic microsatellites for the small brown planthopper *Laodelphax striatellus* (Hemiptera: Delphacidae). *Genet. Mol. Res.* **11**, 1526–1531 (2012).
27. Baldo, L. *et al*. Multilocus sequence typing system for the endosymbiont *Wolbachia pipientis*. *Appl. Environ. Microbiol.* **72**, 7098–7110 (2006).
28. Song, N. & Liang, A. P. Complete mitochondrial genome of the small brown planthopper, *Laodelphax striatellus* (Delphacidae: Hemiptera), with a novel gene order. *Zool. Sci.* **26**, 851–860 (2009).
29. Pritchard, J. K., Stephens, M. & Donnelly, P. Inference of population structure using multilocus genotype data. *Genetics* **155**, 945–959 (2000).
30. Zhang, K. J., Han, X. & Hong, X. Y. Various infection status and molecular evidence for horizontal transmission and recombination of *Wolbachia* and *Cardinium* among rice planthoppers and related species. *Insect Sci.* **20**, 329–344 (2013).
31. Ahrens, M. & Shoemaker, D. Evolutionary history of *Wolbachia* infections in the fire ant *Solenopsis invicta*. *BMC Evol. Biol.* **5**, 35 (2005).
32. Müller, M. J., von Mühlen, C., Valiati, V. H. & Valente, V. L. D. S. *Wolbachia pipientis* is associated with different mitochondrial haplotypes in natural populations of *Drosophila willistoni*. *J. Invertebr. Pathol.* **109**, 152–155 (2012).
33. Franklin, M. T., Ritland, C. E. & Myers, J. H. Genetic analysis of cabbage loopers, *Trichoplusia ni* (Lepidoptera: Noctuidae), a seasonal migrant in western North America. *Evol. Appl.* **4**, 89–99 (2011).
34. Matsumoto, Y. *et al*. Mitochondrial cox sequences of *Nilaparvata lugens* and *Sogatella furcifera* (Hemiptera, Delphacidae): low specificity among Asian planthopper populations. *Bull. Entomol. Res.* **103**, 382–392 (2013).
35. Chapuis, M. P., Plantamp, C., Blondin, L., Vassal, J. M. & Lecoq, M. Demographic processes shaping genetic variation of the solitarious phase of the desert locust. *Mol. Ecol.* **23**, 1749–1763 (2014).
36. Meng, X. F., Shi, M. & Chen, X. X. Population genetic structure of *Chilo suppressalis* (Walker) (Lepidoptera: Crambidae): strong subdivision in China inferred from microsatellite markers and mtDNA gene sequences. *Mol. Ecol.* **17**, 2880–2897 (2008).
37. Peterson, M. A. & Denno, R. F. The influence of dispersal and diet breadth on patterns of genetic isolation by distance in phytophagous insects. *Am. Nat.* **152**, 428–446 (1998).
38. Avise, J. C., Neigel, J. E. & Arnold, J. Demographic influences on mitochondrial DNA lineage survivorship in animal populations. *J. Mol. Evol.* **20**, 99–105 (1984).
39. Raymond, L., Plantegenest, M. & Vialatte, A. Migration and dispersal may drive to high genetic variation and significant genetic mixing: the case of two agriculturally important, continental hoverflies (*Episyrphus balteatus* and *Sphaerophoria scripta*). *Mol. Ecol.* **22**, 5329–39 (2013).
40. Duran, S., Palacin, C., Becerro, M. A., Turon, X. & Giribet, G. Genetic diversity and population structure of the commercially harvested sea urchin *Paracentrotus lividus* (Echinodermata, Echinoidea). *Mol. Ecol.* **13**, 3317–3328 (2004).
41. Broquet, T., Yearsley, J., Hirzel, A. H., Goudet, J. & Perrin, N. Inferring recent migration rates from individual genotypes. *Mol. Ecol.* **18**, 1048–1060 (2009).
42. Hall, L. A. *et al*. Characterizing dispersal patterns in a threatened seabird with limited genetic structure. *Mol. Ecol.* **18**, 5074–5085 (2009).
43. Berry, O., Tocher, M. D. & Sarre, S. D. Can assignment tests measure dispersal? *Mol. Ecol.* **13**, 551–561 (2004).
44. Toews, D. P. & Brelsford, A. The biogeography of mitochondrial and nuclear discordance in animals. *Mol. Ecol.* **21**, 3907–30 (2012).
45. Ballard, J. W. O., Melvin, R. G., Katewa, S. D. & Maas, K. Mitochondrial DNA variation is associated with measurable differences in life-history traits and mitochondrial metabolism in *Drosophila simulans*. *Evolution* **61**, 1735–1747 (2007).
46. Cheviron, Z. A. & Brumfield, R. T. Migration-selection balance and local adaptation of mitochondrial haplotypes in rufous-collared sparrows (*zonotrichia capensis*) along an elevational gradient. *Evolution* **63**, 1593–1605 (2009).
47. Larmuseau, M., Raeymaekers, J., Hellemans, B., Van Houdt, J. & Volckaert, F. Mito-nuclear discordance in the degree of population differentiation in a marine goby. *Heredity* **105**, 532–542 (2010).
48. Pagès, M. *et al*. Cytonuclear discordance among Southeast Asian black rats (*Rattus rattus* complex). *Mol. Ecol.* **22**, 1019–1034 (2013).
49. Ribeiro, Â. M., Lloyd, P. & Bowie, R. C. A tight balance between natural selection and gene flow in a southern african arid-zone endemic bird. *Evolution* **65**, 3499–3514 (2011).
50. Denno, R. F., Roderick, G. K., Olmstead, K. L. & Dobel, H. G. Density-related migration in planthoppers (Homoptera: Delphacidae): The role of habitat persistence. *Am. Nat.* **138**, 1513–1541 (1991).
51. Gong, Z. T. *et al*. The temporal-spatial distribution of domestic rice in ancient China and its implications. *Chin. Sci. Bull.* **52**, 562–567 (2007).
52. Huang, Z. G. & Zhang, W. Q. The origin and expansion of cultivated rice in ancient China. *Trop. Geogr.* **22**, 76–79 (2002).
53. Brand, M. D. The proton leak across the mitochondrial inner membrane. *Biochim. Biophys. Acta-Bioenerg.* **1018**, 128–133 (1990).
54. Ballard, J. W. O. & Pichaud, N. Mitochondrial DNA: more than an evolutionary bystander. *Funct. Ecol.* **28**, 218–231 (2014).
55. Katewa, S. D. & Ballard, J. W. O. Sympatric *Drosophila simulans* flies with distinct mtDNA show difference in mitochondrial respiration and electron transport. *Insect Biochem. Mol. Biol.* **37**, 213–222 (2007).
56. Ruiz-Pesini, E., Mishmar, D., Brandon, M., Procaccio, V. & Wallace, D. C. Effects of purifying and adaptive selection on regional variation in human mtDNA. *Science* **303**, 223–226 (2004).
57. Kazancıoğlu, E., & Arnqvist, G. The maintenance of mitochondrial genetic variation by negative frequency-dependent selection. *Ecol. Lett.* **17**, 22–27 (2014).
58. Zheng, J., Yin, Y. & Li, B. A new scheme for climate regionalization in China. *ACTA Geogr. Sin.* **65**, 3–12 (2010).
59. Sun, J. T., Zhang, Y. K., Ge, C. & Hong, X. Y. Mining and characterization of sequence tagged microsatellites from the brown planthopper *Nilaparvata lugens*. *J. Insect. Sci.* **11**, 134 (2011).

60. Benjamini, Y. & Hochberg, Y. Controlling the false discovery rate: a practical and powerful approach to multiple testing. *J. R. Stat. Soc. Ser. A-Stat. Soc.* **57**, 289–300 (1995).
61. Chapuis, M. P. & Estoup, A. Microsatellite null alleles and estimation of population differentiation. *Mol. Biol. Evol.* **24**, 621–631 (2007).
62. Zhou, W., Rousset, F. & O'Neill, S. Phylogeny and PCR–based classification of *Wolbachia* strains using wsp gene sequences. *Proc. R. Soc. B* **265**, 509–515 (1998).
63. Tajima, F. Statistical method for testing the neutral mutation hypothesis by DNA polymorphism. *Genetics* **123**, 585–95 (1989).
64. Fu, Y. X. Statistical tests of neutrality of mutations against population growth, hitchhiking and background selection. *Genetics* **147**, 915–25 (1997).
65. Rogers, A. R. & Harpending, H. Population growth makes waves in the distribution of pairwise genetic differences. *Mol. Biol. Evol.* **9**, 552–569 (1992).
66. Hedrick, P. W. Perspective: highly variable loci and their interpretation in evolution and conservation. *Evolution* **53**, 313–318 (1999).
67. Meirmans, P. G. Using the AMOVA framework to estimate a standardized genetic differentiation measure. *Evolution* **60**, 2399–2402 (2006).
68. Hubisz, M. J., Falush, D., Stephens, M. & Pritchard, J. K. Inferring weak population structure with the assistance of sample group information. *Mol. Ecol. Resour.* **9**, 1322–1332 (2009).

Acknowledgments

We thank Da-Song Chen, Zi-Wei Song and Wen-Chao Zhu of the Department of Entomology, Nanjing Agricultural University (NJAU) for help with the collection of SBPH. We are also grateful to Dr. Feng Zhang of the Department of Entomology, NJAU for their kind help with data analyses. We thank Peter Biggins (CIRAD Scientific and Technical Information Service) for careful English language editing. This work was supported by a grant-in-aid from the National Key Basic Research Program (973 Program, No. 2009CB119200) from the Ministry of Science and Technology of China, a grant-in-aid (No. 200903051) from the Science and Technology Research Program of the National Agricultural Public Welfare Fund from the Ministry of Agriculture of China and a grant-in-aid from the Specialized Research Fund for the Doctoral Program of Higher Education (SRFDP) from the Ministry of Education of China (Priority Development Area, 20110097130005).

Author contributions

Conceived and designed the experiments: J.T.S. and X.Y.H. Performed the experiments: J.T.S., M.M.W., X.Y.J., Y.K.Z., C.G. and X.M.Y. Analyzed the data: J.T.S., M.P.C., G.H. and X.F.X. Wrote the paper: J.T.S., M.P.C. and X.Y.H.

Additional information

Data Accessibility: GPS values of the sampling locations, microsatellite genotype data, data matrix of the concatenated partial *COI* and COII gene sequences from 1323 individuals, and the 107 haplotype sequences of the concatenated partial *COI* and COII gene sequences are all deposited at Dryad (Doi:10.5061/dryad.66jr2, http://datadryad.org/review?wfID=36983&token=18a66b98-ad73-4dc2-90e0-850da33cd7d7).

Supplementary information accompanies this paper at http://www.nature.com/scientificreports

Competing financial interests: The authors declare no competing financial interests.

How to cite this article: Sun, J.-T. *et al.* Evidence for high dispersal ability and mito-nuclear discordance in the small brown planthopper, *Laodelphax striatellus*. *Sci. Rep.* **5**, 8045; DOI:10.1038/srep08045 (2015).